

Study of the Incompressible Turbulent Boundary Layer with Pressure Gradient

PAUL A. LIBBY,* PAOLO O. BARONTI,† AND LUIGI NAPOLITANO‡

General Applied Science Laboratories, Inc., Westbury, N. Y.

The classical problem of the turbulent boundary layer in incompressible flow with streamwise pressure gradient is considered with a view toward establishing a method that is convenient for practical application and that is based on recent advances in understanding the structure of turbulent layers. Indeed, a two-layer model of the boundary layer is assumed with the flow in the inner layer given by the law of the wall and in the outer layer by a flow with wakelike characteristics. The general analysis is first developed and then applied to equilibrium and near-equilibrium flows. The predictions of the analysis are compared to available data for several such flows corresponding to adverse, zero, and favorable pressure gradients and are shown to be in satisfactory agreement therewith. Several numerical experiments generating additional equilibrium flows are performed. The implication of these results with respect to the application of this study to nonequilibrium flows is discussed.

Nomenclature

A	= constant in law of the wall, taken here to be 2.43
b	= constant in law of the wall, taken here to be 7.5
C_1	= constant, cf. Eq. (6)
f	= velocity profile in terms of law of the wall, u/v^*
F	= velocity profile in terms of the velocity defect, $[(u/u_e) - 1]\varphi$
H_e	= form factor, δ^*/θ
L	= arbitrary reference length
p	= static pressure
R	= Reynolds number based on boundary-layer thickness, $u_e \delta/\nu$
R_L	= Reynolds number based on the reference length, $u_e L/\nu$
R_x	= Reynolds number based on streamwise coordinate, $u_e x/\nu$
S	= profile parameter, T_2/T_1
T_1, T_2	= parameters in the shear-stress profile, cf. Eqs. (7) and (8)
u	= streamwise velocity component
U	= normalized external velocity, u_e/u_{e0}
v	= velocity component normal to surface
v^*	= shearing velocity, $(\tau_w/\rho)^{1/2}$
x	= streamwise coordinate
x_i	= initial streamwise length
y	= coordinate normal to the surface
α	= transformed normal coordinate, yv^*/ν
β	= constant in description of the eddy viscosity, cf. Eqs. (18) and (19)
δ	= boundary-layer thickness
δ^*	= boundary-layer displacement thickness
ϵ_0	= eddy viscosity in the outer layer
η	= normalized normal coordinate, y/δ
ν	= kinematic viscosity
ξ	= normalized streamwise coordinate, $(x - x_i)/L$
π	= wake parameter of Coles
ρ	= mass density

Σ	= normalized momentum thickness, θ/δ
τ	= shear stress
φ	= normalized external velocity, u/v^*
Ω	= normalized displacement thickness, δ^*/δ

Subscripts

1	= conditions at the interface of the two layers
e	= conditions external to the boundary layer
$e, 0$	= conditions external to the boundary layer at a reference station, usually at $\xi = 0$
s	= conditions at edge of the laminar sublayer
w	= conditions at the wall ($y = 0$)

I Introduction

AS part of a general investigation of boundary-layer problems connected with the inlet of hypersonic, air-breathing vehicles, a detailed study of the turbulent boundary layer in incompressible flow with streamwise pressure gradient has been undertaken. The consideration of the incompressible case is justified as a first and fundamental step in the treatment of the practical problem by the availability of transformation techniques that reduce to a large extent the description of the compressible case to an incompressible form.

The problem of the turbulent boundary layer in incompressible flow with adverse pressure gradient is classical (cf., e.g., Ref. 1). Prior to roughly 1955, the analysis of such flows involved the semiempirical correlation of one or more shape parameters that were judged to represent the velocity profiles. Accordingly, such analyses were of doubtful validity beyond the range of conditions represented by the correlations. However, in the mid 1950's there appeared a series of papers¹⁻⁶ that were written by several investigators and that provided a somewhat firmer basis for analyses of the turbulent boundary layer; in these analyses empiricism is still present, as would be expected in view of the current inadequate knowledge of the details of turbulent shear flows, but is kept at a more fundamental level. Although the treatments of these workers differ in detail and in point of view, there is general agreement that the turbulent boundary layer for a wide class of flows can be characterized by an inner region in which the well-known law of the wall applies and an outer region of wakelike character. The existence of these two layers is associated with the different response to shear and to pressure gradient by the fluid near the wall from that by the fluid near the external flow.

An important aspect of the recent analyses of turbulent flows is the concept of equilibrium layers due to Clauser¹

Received May 6, 1963; revision received November 20, 1963. The research reported here was supported by Republic Aviation Corporation under Extension Agreement dated February 1, 1963. The authors are pleased to acknowledge that Antonio Ferri suggested this study, that Joseph A. Schetz and Paul A. Taub provided stimulating discussion, and that Leatrice Groffman carried out the numerical computations.

* Senior Scientific Investigator; also Professor of Aerospace Engineering, Polytechnic Institute of Brooklyn, Freeport, N. Y. Member AIAA.

† Senior Scientist.

‡ Formerly Senior Scientific Investigator; now Director of the Institute of Aeronautics, University of Naples, Naples, Italy.

and defined as those for which the velocity profiles in terms of $(u - u)/v^* = F(\eta)$, $\eta = y/\delta$ are invariant in the streamwise direction. Clauser established experimentally such profiles for two adverse pressure distributions and showed in Ref. 2 that such flows can be analyzed in terms of an outer region in which the eddy viscosity, as in wakes, is essentially constant in the normal, i.e., y , direction. The concomitant theoretical analysis of Clauser involved obtaining solutions to the laminar boundary-layer equations in similar form with the kinetic viscosity ν interpreted as a turbulent eddy viscosity and with slip at the wall, i.e., $u(0) \neq 0$. The resulting "laminar" profiles were matched to the law of the wall so as to make the velocity and shear continuous at the interface of the two layers. It was found that the eddy viscosity in the outer layer (denoted here as ϵ_0) was roughly expressible for a variety of flows in terms of $\beta \equiv \epsilon_0/u \delta^*$, with $\beta \approx 0.018$. Coles⁴ later showed that many flows evoking practical interest and involving favorable and adverse pressure gradients may be considered to be near equilibrium, i.e., to involve velocity profiles in terms of $(u - u)/v^*$ which slowly change with x . In addition, he proposed an explicit velocity profile representing a linear combination of the law of the wall and a universal law of the wake; the multiplicative factor before the law of the wake was denoted $\pi(x)$, which for equilibrium profiles in the sense of Clauser is a constant. Coles did not explicitly invoke the wakelike character of the outer layer with respect to the uniformity in the normal direction of the eddy viscosity therein and did not put his analysis in the form for application to practical problems. However, his demonstration of the computation of the shear stress in the inner layer from the law of the wall plays an essential role in the present analysis.†

Ferrari⁶ has presented a detailed study of turbulent boundary layers. Of particular interest in the present study is the treatment of the turbulent layer with streamwise pressure gradient. Again, there is employed a two-layer model with a modified law of the wall and an outer region with an eddy viscosity dependent only on the streamwise coordinate. However, the actual description for the eddy viscosity is derived from a consideration of the turbulent energy in the outer region and is considerably more involved than that obtained by Clauser.

Recently, Rotta⁹ has provided a comprehensive review of the turbulent boundary layer including discussions of the mechanisms involved and of the existing calculation procedures for equilibrium and general flows.

In this report several of the ideas of the forementioned authors have been combined in order to establish a method that can be conveniently employed in high-speed computers to the analysis of turbulent boundary-layer problems with streamwise pressure gradients. These ideas will be discussed as they are employed. It is noted at the outset that this analysis, when applied to flows with adverse pressure gradients sufficiently strong so as to cause separation, can give a strong but not unequivocal indication of separation. This is because of the assumption of the law of the wall in the inner region; in the neighborhood of separation this law does not apply, and, accordingly, the present analysis will fail. However, as separation is approached, the shearing velocity v^* must approach zero, $\varphi \equiv u/v^* \rightarrow \infty$, and, in general, a strong indication of separation could be expected. This shortcoming has its counterpart in previous analyses wherein specific values of the shape parameter, e.g., the form factor, are attributed to the separation point.

In the next section the general analysis is developed. Then equilibrium and near-equilibrium flows are considered; the velocity profiles and boundary-layer characteristics of such

flows as predicted by the theory are compared to experiment for cases of adverse, zero, and favorable pressure gradient. Agreement satisfactory for most purposes is shown. Finally, new equilibrium flows are generated by numerical experiments employing the analysis.

II General Analysis

It is assumed that the mean turbulent boundary layer may be described by the usual boundary-layer equations for laminar flow properly interpreted. Thus, the momentum and mass conservation equations are

$$u \frac{\partial u}{\partial x} + v \frac{\partial u}{\partial y} = u \frac{du_e}{dx} + \frac{1}{\rho} \frac{\partial \tau}{\partial y} \quad (1)$$

$$\frac{\partial u}{\partial x} + \frac{\partial v}{\partial y} = 0 \quad (2)$$

Consider now a two-layer model of the boundary layer; let $\delta = \delta(x)$ be the distribution of boundary-layer thickness, which is divided into two regions corresponding to $0 < \eta \leq \eta_1$ and to $\eta_1 < \eta \leq 1$, where $\eta = y/\delta$. In the inner region let the law of the wall apply, so that

$$\begin{aligned} u/u &= \eta R/\varphi^2 & 0 < \eta < \eta_1 \\ &= (A/\varphi) \ln(Rb\eta/\varphi) & \eta_1 < \eta < 1 \end{aligned} \quad (3)$$

where A and b are known constants taken in the numerical work here to be those of Clauser,¹ namely, $A = 2.43$, $b = 7.5$.

It is the immediate objective of the analysis to construct a velocity profile for the outer layer in which the eddy viscosity is assumed to be constant.** To do so, it is necessary to develop a shear-stress profile. In the past, such profiles have been assumed in turbulent boundary-layer theory in the form of polynomials satisfying boundary conditions at the wall and at the outer edge. Rotta⁹ has recently reviewed this procedure and has shown that such profiles can be in considerable error in the region wherein the law of the wall applies. This observation suggests that some of the errors associated with the assumption of a shear profile applicable from the wall to the outer edge can be reduced by following Coles,¹⁰ in that the shear and its derivative with respect to η at the interface $\eta = \eta_1$ are computed from Eqs. (1) and (3). Thus, a polynomial representation for the shear must be applied only in the outer region.

Shear Stress in the Inner Layer

It is possible to show (cf., e.g., Coles¹⁰ or Rotta⁹) that within the inner layer

$$\tau = \tau_w + \left(\frac{dp}{dx} \right) y + \mu \frac{dv^*}{dx} \int_0^{yv^*/\nu} f^2(\alpha) d\alpha \quad (4)$$

where f is implied by Eqs. (3) to be

$$\begin{aligned} f &\equiv u/v^* = \alpha & 0 < \alpha \leq \alpha \\ &= A \ln b\alpha & \alpha > \alpha \end{aligned} \quad (5)$$

and where α is defined by the requirement of continuity in f at the juncture; with the values of A and b employed here, $\alpha \equiv yv^*/\nu = 10.6$.

Substitution of Eqs. (5) into Eq. (4) results, after considerable rearrangement, in the following convenient form:

$$\begin{aligned} \frac{\tau}{\tau_w} &= 1 - \left(\nu \frac{R\varphi^2}{u^2} \frac{du_e}{dx} \right) \eta + A^2 \frac{\nu R}{u} \left[\frac{1}{u_e} \frac{du_e}{dx} - \frac{1}{\varphi} \frac{d\varphi}{dx} \right] \times \\ &\quad \left\{ \eta \left[\ln^2 \left(\frac{Rb\eta}{\varphi} \right) - 2 \ln \left(\frac{Rb\eta}{\varphi} \right) + 2 \right] + \frac{C_1 \varphi}{A^2 R} \right\} \end{aligned} \quad (6)$$

† It is recognized that this concept applies to flows with local Reynolds numbers greater than a certain minimum (cf. Ref. 7).

‡ A similar computation has been given by Spence.⁸

** Note that in a "refined" analysis the intermittance in the outer portion of the boundary layer could be considered so that ϵ_0 would decrease as $\eta \rightarrow 1$.

where for the present analysis $C_1 = -375$ and where $\eta_* \leq \eta \leq \eta_1$ ††

Differentiate Eq (6) with respect to η , and set $\eta = \eta_1$; let

$$\begin{aligned} T_1 &\equiv \left(\frac{\tau}{\tau_w} \right) \bigg|_{\eta=\eta_1} \\ T_2 &\equiv \frac{\partial}{\partial \eta} \left(\frac{\tau}{\tau_w} \right) \bigg|_{\eta=\eta_1} \end{aligned} \quad (7)$$

It is found that

$$T_2 = - \frac{\nu R \varphi^2}{u^2} \frac{du_e}{dx} + \frac{A^2 \nu R}{u} \left(\frac{1}{u} \frac{du_e}{dx} - \frac{1}{\varphi} \frac{d\varphi}{dx} \right) \ln^2 \left(\frac{Rb\eta_1}{\varphi} \right) \quad (8)$$

Thus, the shear and its gradient at $\eta = \eta_1$ have been obtained from the law of the wall

Shear Stress in the Outer Region

Now in the outer region assume a polynomial representation for the shear-stress distribution so that, at $\eta = \eta_1$,

$$\begin{aligned} \tau/\tau_w &= T_1 \\ (\partial/\partial \eta)(\tau/\tau_w) &= T_2 \end{aligned} \quad (9)$$

and at $\eta = 1$,

$$\tau/\tau_w = (\partial/\partial \eta)(\tau/\tau_w) = 0$$

Then

$$\begin{aligned} \frac{\tau}{\tau_w} &= \frac{T_1}{(1-\eta_1)^3} [(1-3\eta_1) + (6\eta_1)\eta - 3(1+\eta_1)\eta^2 + 2\eta^3] + \\ &\frac{T_2}{(1-\eta_1)^2} [(-\eta_1) + (1+2\eta_1)\eta - (2+\eta_1)\eta^2 + \eta^3] \end{aligned} \quad (10)$$

which expresses the shear-stress profile with T_1 , T_2 , and η_1 as parameters

It is noted here that no free parameter has been retained in the shear profile given by Eq (10). To do so would necessitate an additional describing equation, which could be obtained by applying the method of moments as was done by Tetervin and Lin¹¹. In the past the difficulty associated with such methods, when applied to turbulent flows, has been related to the problem of assuming, simultaneously, reasonable shear and velocity profiles. However, since the present approach is based on the two-layer model of the turbulent layer and results in an intimate relation between these two profiles, a refinement of the present approach employing a first moment equation would be straightforward and might be of interest.

Velocity Profile in the Outer Region

In accordance with the two-layer model of the turbulent boundary layer, the outer region is assumed to be of wake-like character and thus to have an eddy kinematic viscosity, which is denoted by ϵ_0 , which is uniform with respect to y but which can vary with the streamwise coordinate x . Then the velocity profile can be obtained by integrating the equation

$$\tau = \rho \epsilon_0 (\partial u / \partial y) \quad (11)$$

which can be written more conveniently as

$$\left(\frac{R\nu}{\epsilon_0 \varphi} \right) \frac{\tau}{\tau_w} = \varphi \frac{\partial}{\partial \eta} \left(\frac{u}{u_e} \right) \quad (12)$$

†† It is interesting to note that in the usual polynomial assumption for a shear profile only the first two terms in the right-hand side of Eq (6) are retained

It is assumed now that ϵ_0 is continuous at $\eta = \eta_1$, although no requirement on $\partial \epsilon_0 / \partial \eta$ is specified. Accordingly, Eqs (3, 7, and 12) yield

$$R\nu/\epsilon_0 \varphi = A/T_1 \eta_1 \quad (13)$$

Furthermore, if Eq (10) is substituted into Eq (12), if the result is integrated once with respect to η , and if $u/u_e = 1$ at $\eta = 1$ for all x , there results

$$\begin{aligned} \left(\frac{u}{u_e} - 1 \right) \varphi &= - \frac{R\nu}{\epsilon_0 \varphi} \int_{\eta}^1 \left(\frac{\tau}{\tau_w} \right) d\eta' \\ &= - \frac{A}{\eta_1(1-\eta_1)^2} \left\{ \frac{1}{(1-\eta_1)} \left[\left(\frac{1}{2} - \eta_1 \right) - \right. \right. \\ &\quad \left. \left. (1-3\eta_1)\eta - (3\eta_1)\eta^2 + (1+\eta_1)\eta^3 - \frac{1}{2}\eta^4 \right] + \right. \\ &\quad \left. \frac{T_2}{T_1} \left[\left(\frac{1}{12} - \frac{\eta_1}{3} \right) + (\eta_1)\eta - \left(\frac{1}{2} + \eta_1 \right) \eta^2 + \right. \right. \\ &\quad \left. \left. \left(\frac{2}{3} + \frac{\eta_1}{3} \right) \eta^3 - \frac{\eta^4}{4} \right] \right\} \end{aligned} \quad (14)$$

which is the desired velocity profile in the outer region. The quotient T_2/T_1 will be a significant parameter in the analysis and will thus be denoted S , i.e., $S \equiv T_2/T_1$. Note that in the outer region

$$[(u/u_e) - 1] \varphi = fcn(\eta, \eta_1, S)$$

Thus, η_1 and S serve as profile parameters; it will be shown below that these two parameters are related.

Velocity Matching Condition and Its Implications

In the preceding analysis the shear stress, its gradient, and the eddy viscosity have been made continuous at $\eta = \eta_1$, i.e., at the interface between the two layers. Require now that the velocity be continuous; then from Eqs (3) and (14) applied at $\eta = \eta_1$ there is obtained

$$A \ln \left(\frac{Rb\eta_1}{\varphi} \right) - \varphi = - \frac{A(1-\eta_1)}{2\eta_1} \left[1 + S \left(\frac{1-\eta_1}{6} \right) \right] \quad (15)$$

which represents a skin-friction law in the form $fcn(\varphi, R, \eta_1, S) = 0$. The implications of this equation will be discussed in some detail below.

Equation (15) can be employed to rewrite the equation for the velocity profile in the inner layer; Eqs (3) can be arranged as

$$\left(\frac{u}{u_e} - 1 \right) \varphi = -\varphi + A \ln \left(\frac{Rb\eta_1}{\varphi} \right) + A \ln \left(\frac{\eta}{\eta_1} \right) \quad (3a)$$

so that from Eq (15)

$$\left(\frac{u}{u_e} - 1 \right) \varphi = A \ln \left(\frac{\eta}{\eta_1} \right) - \frac{A(1-\eta_1)}{2\eta_1} \left[1 + S \left(\frac{1-\eta_1}{6} \right) \right] \quad (3b)$$

Thus, the inner velocity profile when matched to the outer layer results in

$$[(u/u_e) - 1] \varphi = fcn(\eta, \eta_1, S)$$

An examination of Eqs (14) and (3b) indicates that, if S and η_1 are independent of x for a particular flow, then the velocity profile in both layers can be represented by

$$[(u/u_e) - 1] \varphi \equiv F(\eta)$$

and the flow by definition would be an equilibrium flow.

Thus, according to this analysis, an equilibrium profile is defined by a pair of values η_1 and S . It is important to note that, if S and η_1 are constants, the shear-stress profile, which depends on T_1 and T_2 explicitly, is not necessarily invariant

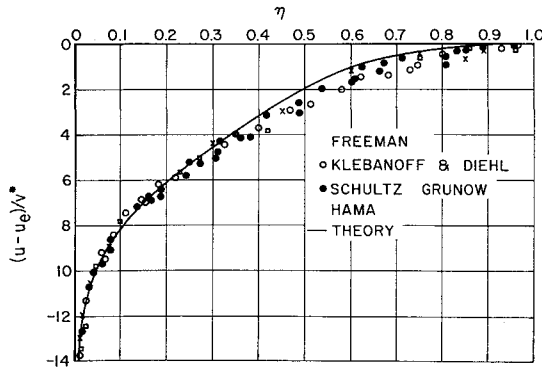


Fig 1 Velocity profiles for constant-pressure flow (data from Ref 1)

with respect to the streamwise coordinate. As has been noted by Clauser,² the concept of an equilibrium flow does not apply to all features of the boundary layer; in particular, he indicates that, if the velocity profile is exactly an equilibrium one, then the shear-stress distribution will not quite be invariant.

Return now to the skin-friction law, which is given by Eq (15) and which is not complete unless S and η_1 are specified. It is worthwhile at this juncture to assume that there exists a functional form $\eta_1 = \eta_1(S)$ corresponding to physically acceptable flows; then a skin-friction law corresponding to that given by Ludwig and Tillman¹² can be obtained as follows. With the velocity profiles expressed as Eqs (3b) and (14), the form factor H becomes

$$H \equiv \frac{\int_0^1 \left[1 - \left(\frac{u}{u_e} \right) \right] d\eta}{\int_0^1 \left(\frac{u}{u_e} \right) \left[1 - \left(\frac{u}{u_e} \right) \right] d\eta} = \frac{\varphi \int_0^1 F d\eta}{\int_0^1 F^2 d\eta + \varphi \int_0^1 F d\eta} \quad (16)$$

Thus, Eq (16) implies $H_e = H(\varphi, S, \eta_1)$, so that with the postulated additional relation between S and η_1 the skin-friction law of Eq (15) can be put in the form $\varphi = \varphi(R, H)$, as in Ref 12 ‡. It is of interest to note that with the postulated relation $\eta_1 = \eta_1(S)$ the parameter S in the present analysis is a shape parameter analogous to that employed in the past, but of course arising from the two-layer model and not related in a simple fashion to the gradient of external velocity.

Momentum Integral

The foregoing discussion has provided the desired velocity profiles in the inner and outer layers. An analysis em-

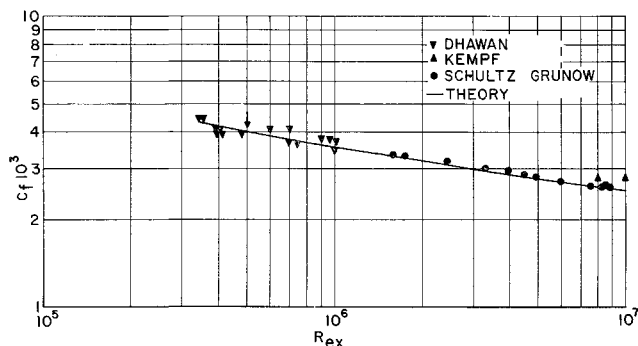


Fig 2 Variation of local skin-friction coefficient for constant-pressure flow (data from Ref 14)

‡ Although no simple functional relation of the sort provided by Ref 12 is given by the present analysis, the results given here are in good quantitative agreement with those of Ref 12 over the entire range of H considered there.

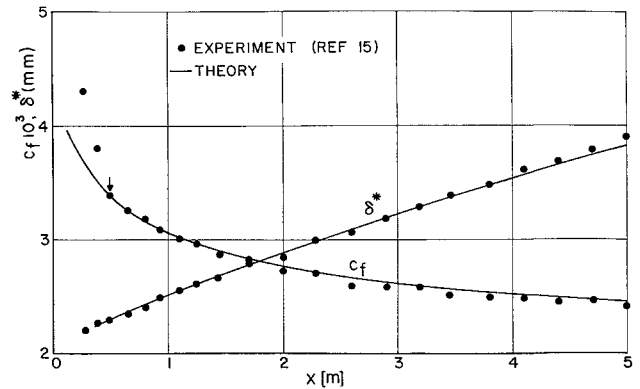


Fig 3 Distribution of boundary-layer characteristics for a constant-pressure flow; $u_e = 33$ m/sec

ploying these profiles requires the momentum integral equation derived from Eq (1) integrated across the boundary-layer thickness. In terms of the variables under consideration, this can conveniently be written as §§

$$\frac{1}{R} \frac{dR}{d\xi} + \frac{1}{\Sigma} \frac{d\Sigma}{d\xi} + \frac{1}{u_e} \frac{du_e}{d\xi} \left(1 + \frac{\Omega}{\Sigma} \right) = \left(\frac{u_e L}{\nu} \right) \frac{1}{\varphi^2 R \Sigma} \quad (17)$$

where

$$\xi = (x - x_i)/L$$

$$\Sigma \equiv \int_0^1 \frac{u}{u_e} \left[1 - \frac{u}{u_e} \right] d\eta = \Sigma(\varphi, \eta_1, S) = - \left[\varphi^{-2} \int_0^1 F^2 d\eta + \varphi^{-1} \int_0^1 F d\eta \right]$$

$$\Omega = \int_0^1 \left[1 - \frac{u}{u_e} \right] d\eta = \Omega(\varphi, \eta_1, S) = -\varphi^{-1} \int_0^1 F d\eta$$

Completion of the System of Equations: General Discussion

At this stage in the analysis, it is constructive to consider two classes of problems and the dependent variables associated with each. In the direct problem of boundary-layer theory, the velocity distribution $u = u(\xi)$ is given; it is required to find the boundary-layer characteristics described by R , φ , η_1 , and S as functions of ξ . In the inverse problem for an equilibrium flow, a pair of values η_1 and S define a velocity profile; it is required to find the velocity distribution $u_e = u(\xi)$ yielding such a velocity profile and to find the boundary-layer characteristics R and φ as functions of ξ in such a flow. In both classes of problems, Eqs (15) and (17) and the definition of S are applicable and correspond to three equations. For the direct problem, an additional equation is required to complete the system of equations; for the inverse problem, the physically acceptable pairs of values η_1 and S must be determined.

The additional equation for the direct problem can apparently be obtained in several ways within the framework of the present analysis. In particular, a local equilibrium concept can be applied as follows. Assume that there has been established from a consideration of equilibrium flows a spectrum of pairs η_1 and S corresponding to physically acceptable equilibrium profiles. Such a spectrum can be considered to yield a function $\eta_1 = \eta_1(S)$. Now, if it is assumed that a general boundary layer behaves as though locally an equilibrium layer, this function completes the system of equations that yield R , φ , η_1 , and S as functions of ξ .

§§ Only the two dimensional case is considered explicitly here, but the axisymmetric case can be developed without difficulty.

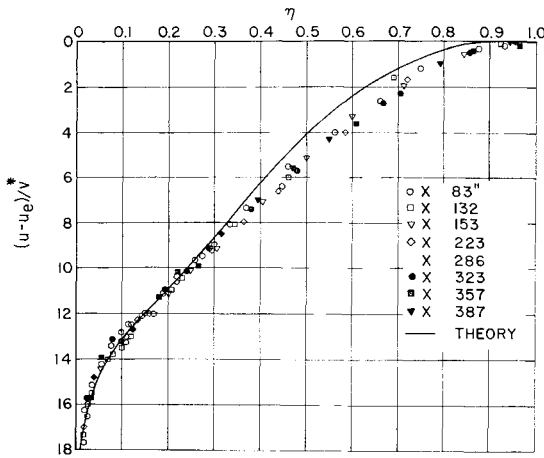


Fig 4 Velocity profiles for adverse pressure gradient: pressure distribution I (data from Ref 1)

In this point of view the function $\eta_1 = \eta_1(S)$ plus the definition of S is analogous to the equation for the shape parameter used in the past in turbulent analysis. An alternative but related means of completing the system of equations is provided by the observation of Clauser² that the eddy viscosity in the outer layer denoted by ϵ_0 is expressible for a variety of equilibrium flows as

$$\epsilon_0 = \beta u \delta^* \quad (18)$$

where $\beta = 0.018$. Note that from Eqs (13) and (18)

$$\beta = T_1 \eta_1 / A \varphi \Omega \quad (19)$$

Again, if this relation is assumed to apply to the general boundary layer, the system of equations is complete. Note that either of the two additional equations would give identical results if the first would yield a distribution of $\beta = \beta(\xi)$ from Eq (19) corresponding to $\beta \approx 0.018$.

In the inverse problem for equilibrium flows, the pairs of values η_1 and S can be determined in two ways. First, the experimental results obtained for equilibrium and near-equilibrium flows provide velocity profiles in the form $[(u/u_e) - 1]\varphi = F(\eta)$. By curve fitting and/or collocation, the values of η_1 and S corresponding thereto can be selected. Thus all of the flows compiled by Coles⁴ can be employed to build up pairs of values. The correctness of these values within the framework of the analysis can be established by comparing the computed distributions of R , φ , and u with the corresponding distributions obtained from experiment. As a by-product of this comparison, the distribution of β can be computed and compared with the value found by Clauser.

It is also possible to construct additional pairs of values η_1 and S by assuming that $\beta \approx 0.018$ ^{††} and by performing a numerical experiment as follows. Assume that at a given station an equilibrium profile corresponding to a pair of values η_1 and S exists and that at this station the boundary-layer thickness related to R is known. Then it is possible to construct theoretically the distributions of R , φ , and u required to maintain this profile in the streamwise direction. In addition, the distribution of β can be computed; a pair of values η_1 and S could be deemed physically acceptable if $\beta \approx 0.018$ for all streamwise stations. Now it will be recognized that, if the initial condition on R is changed while η_1 and S are fixed, then the distributions of R , φ , and u will be altered, but, more important, β may change. However, if in an equilibrium flow the shear profile is only slightly varying, so that both T_1 and T_2 are almost constant, then it would be expected that β , as may be seen from Eq (19),

^{††} As will be seen below, the present analysis suggests a value of $\beta \approx 0.016$.

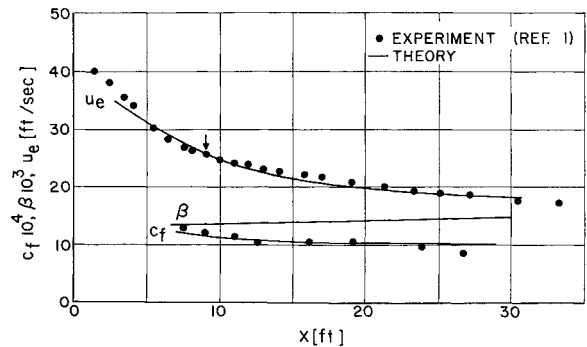


Fig 5 Boundary-layer characteristics for adverse pressure gradient: pressure distribution I

would change only slightly with changes in the numerical experiment.

The remainder of this paper will be concerned primarily with equilibrium flows and with developing a functional form $\eta_1 = \eta_1(S)$ employing both methods described in the foregoing.

III Application to Equilibrium and Near-Equilibrium Flows

Consider now the detailed formulation of the inverse problem for equilibrium flows; assume that a suitable pair of values η_1 and S is selected. Then Eqs (15) and (17) and the equation resulting from the definitions of T_2 , T_1 , and S [cf Eqs (7) and (8)] yield three equations in R , φ , and u_e . In the interests of brevity, these will not be given explicitly^{***}; it will be sufficient to state that they can be formulated for convenience in numerical analysis as three first-order differential equations that were integrated by the Kutta-Runge-Gill procedure on a Bendix G-15 computer and that involve a single parameter R_L . However, the appearance of R_L is somewhat artificial, in that $\xi R_L = R_x$, so that the independent variable could, therefore, be considered R_x . Because of the part algebraic, part differential nature of the defining equations, it is possible to specify only two initial quantities, e.g., the values of u_e (or $U \equiv u/u_e$) and of R at $\xi = 0$ ^{†††}.

Values of S and η_1 from Experimental Data

Consider the procedure employed to select from experimental data on equilibrium and near-equilibrium flows the

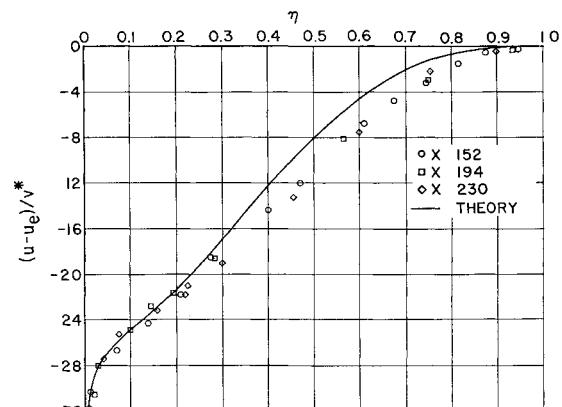


Fig 6 Velocity profiles for adverse pressure gradient: pressure distribution II (data from Ref 1)

^{***} For details of the analysis as well as extended results, see Ref 13, from which this paper was prepared.

^{†††} It is of interest to note that from the point of view adopted herein the flat-plate boundary layer which represents one equilibrium flow, is one yielding $U \approx 1$.

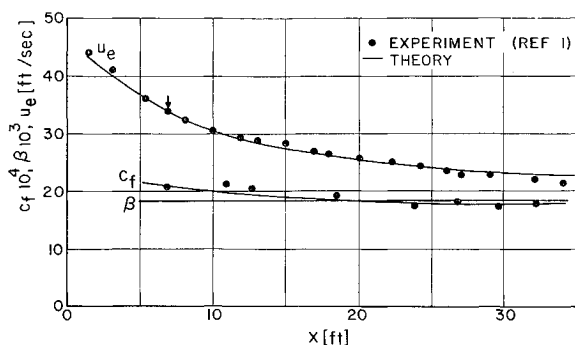


Fig 7 Boundary-layer characteristics for adverse pressure gradient: pressure distribution II

physically acceptable pairs of S and η_1 . The velocity profiles are assumed to be available in the form $[(u/u_e) - 1]\varphi = F(\eta)$. In the region close to the wall, i.e., $\eta \lesssim 0.15$, the log portion of the law of the wall is assumed to apply; this, plus estimates of the quantities appearing in the definition of S , e.g., φ , $d\varphi/dx$, u_e , du_e/dx , permits estimates of a pair of values η_1 and S for a particular experiment to be made. These were adjusted a posteriori to yield agreement between the theoretical and experimental distributions of R , U , and φ , as shown below. In addition, the distributions of β with streamwise coordinate were also computed.

The simplest case of equilibrium flow is the smooth flat plate. For this case, the experimental data provided by a variety of workers as presented by Clauser¹ are shown in Fig 1. Also shown is the theoretical velocity profile corresponding to $S = -0.5$ and $\eta_1 = 0.131$. The satisfactory agreement will be noted. The values of U obtained by integration were unity within a few percent over a wide range of ξ . Moreover, the theoretical skin friction is compared with experimental data presented in Ref 14 as a function of R_x in Fig 2. For these calculations, $R_L = 10^7$, and the initial value of φ was selected from experimental data at one station corresponding to $R_x = 0.5 (10^6)$. Again the agreement is satisfactory. It is noted that the computed values of $\beta = 0.0160 \pm 6(10)^{-5}$ over the entire range of R_x .

The agreement of the velocity profiles shown in Fig 1 and of the distribution of skin friction with x as shown in Fig 2 implies agreement of other flat-plate boundary-layer properties. For example, Fig 3 presents a comparison of the distributions of c_f and δ^* computed by the present analysis with the forementioned values of S and η_1 with the experimental results of Ref 15. The excellent agreement will be noted.

Consider next the equilibrium flow with an adverse pressure gradient denoted as pressure distribution I by Clauser.¹²

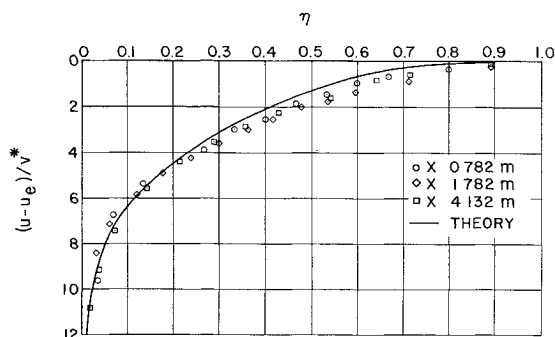


Fig 8 Velocity profiles for favorable pressure gradient: Ludwig and Tillmann channel VII

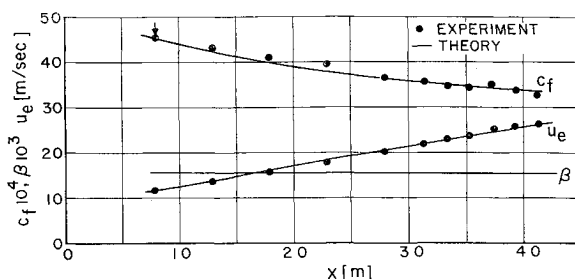


Fig 9 Boundary-layer characteristics for favorable pressure gradient: Ludwig and Tillmann channel VII

The theoretical and experimental velocity profiles are shown in Fig 4; the values of $S = 3.3$ and $\eta_1 = 0.125$ have been found in this case by the procedure just outlined. The integration of the equations for equilibrium flow is initiated at a value of $\xi = 0$ corresponding to $x = 83$ in Clauser's scale and results in the distribution of c_f , u , and β shown in Fig 5. The satisfactory agreement between theory and experiment in all respects will be noted. In particular it is noted that $\beta = 0.0184 \pm 5(10)^{-4}$.

The foregoing calculations have been repeated for the flow identified by Clauser as pressure distribution II; the results permitting comparison between theory and experiments are shown in Figs 6 and 7. Note that the agreement is satisfactory and that $\beta = 0.0147 \pm 5(10)^{-4}$ over the entire range of x .

Two flows involving favorable pressure gradient have also been considered; one has been identified by Coles³ as Ludwig and Tillman channel VII^{§§§}; the second is given by Bauer¹⁶ and is identified as 40° slope.

For the flow identified as channel VII, velocity profiles in terms of $[(u/u_e) - 1]\varphi$ vs η had to be constructed from the experimental data; the results are shown in Fig 8. The values of S and η_1 found for this profile are $S = -2.4$, $\eta_1 = 0.113$ and yield the streamwise distributions of boundary layer characteristics shown in Fig 9. The value of β will be seen to be roughly constant, i.e., $\beta = 0.0155 \pm 5(10)^{-4}$.

Again, for the flow corresponding to favorable pressure gradient and denoted as Bauer 40° slope,¹⁶ the velocity profiles as shown in Fig 10 had to be constructed from the experimental data. The values of S and η_1 , corresponding to these data, were found to be $S = -2.0$, $\eta_1 = 0.12$ and yield the distribution of boundary-layer characteristics as shown in Fig 11. In particular, it is seen that $\beta = 0.016 \pm 5(10)^{-4}$. In both of these flows with favorable pressure gradient, the comparison between theory and experiment is quite satisfactory.

The pertinent results with respect to the flows considered are summarized in Table 1. Note that the values of the

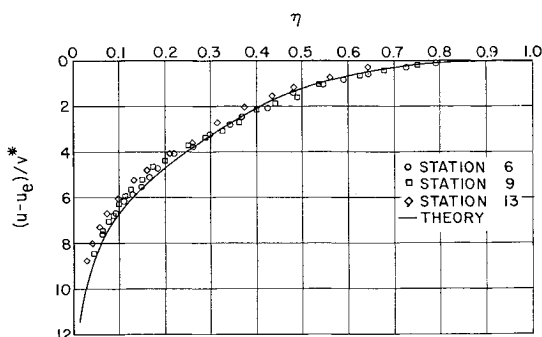


Fig 10 Velocity profiles for favorable pressure gradient: Bauer 40° slope¹⁶

††† An arrow is shown on this and subsequent figures where the numerical integration is initiated

§§§ The authors are indebted to D. Coles for supplying the experimental data for this flow

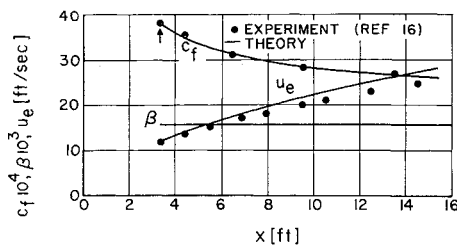


Fig 11 Boundary-layer characteristics for favorable pressure gradient: Bauer 40 slope

integral

$$- \int_0^1 F dy$$

computed from the theoretical profiles with the selected values of η_1 and S are also given; this integral is frequently considered a profile parameter $\int_0^1 F dy$. It will be noted that the values here are in satisfactory agreement with the corresponding values from experiment and from other analyses (cf Refs 2-4 and 9), as would be expected from the agreement of the velocity profiles shown in Figs 1, 4, 6, 8, and 10. The pairs of values η_1 and S are plotted in Fig 12.

It is also of interest to note that the observed relative constancy of β with streamwise distance implies that the shear profile parameter T_1 is also almost constant [cf Eq (19)]. Accordingly, the shear stress profiles in terms of τ/τ_w vs η are almost invariant in an equilibrium flow according to this analysis.

Values of S and η_1 Generated by Numerical Analysis

Consider now the numerical experiments leading to additional, physically acceptable pairs of values η_1 and S . It was necessary to consider first the influence of the initial boundary-layer thickness R_0 , i.e., the value of R at $\xi = 0$, on the computed distributions of β . For this purpose, two cases, one of strong adverse and the other of strong favorable pressure gradient, were considered. The procedure followed was as follows. For a particular value of R_0 , a pair of values η_1 and S was selected so that $\beta \cong 0.016$ over the range of $0 < \xi < 1$. Since R_L was taken to be 10^7 , this range represents a considerable range in R_x . Note that this particular value of β was selected, since the results shown in Table 1 indicate somewhat better agreement between the results of the present analysis and experiment for this value than

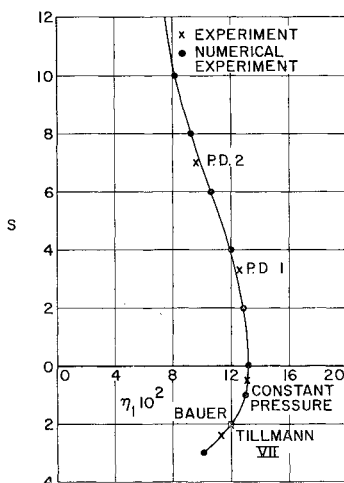


Fig 12 Relation between profile parameters η_1 and S

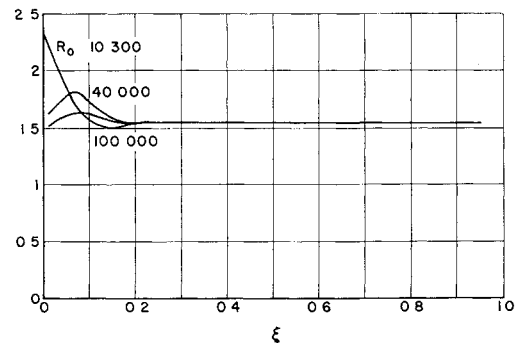


Fig 13 Effect of initial boundary-layer thickness on eddy viscosity parameter: numerical experiment for strong adverse pressure gradient ($\eta_1 = 0.081$, $S = 10$)

for the value of 0.018 found by Clauser. With a pair η_1 , S so selected, R_0 was then changed and the resulting distribution of R , φ , U , and in particular β computed.

A typical result of this study is shown in Fig 13, which applies to a flow with a strong adverse gradient. It will be noted that over a tenfold range of R_0 the computed distribution of β for a pair of values considered acceptable is altered only in the range of $\xi \ll 1$. Similar results apply for a flow with a strong favorable pressure gradient.**** Since for flow with zero pressure gradient the value of β is independent of R_0 , it appears that the numerical experiments under consideration lead to pairs of values η_1 and S , essentially independent of R_0 .

Such pairs have been computed for a range of S as shown in Fig 12. It will be noted that a single functional relation $\eta_1 = \eta_1(S)$ can be inferred from both the experimental and numerical results.

Concluding Remarks Concerning Equilibrium Layers

The results of this section indicate that the suggestion of Clauser² concerning the form for the eddy viscosity in the outer layer in conjunction with the present analysis provides a means for describing, with relative simplicity and accuracy, the characteristics of equilibrium boundary layers, both with

Table 1 Summary of the computed values of β , S , η_1 , and $-\int_0^1 F d\eta$

Flow	β	S	η_1	$-\int_0^1 F d\eta$
Ludwig and Tillman				
channel VII	$0.0155 \pm 5(10)^{-4}$	-2.4	0.113	2.31
Bauer 40 slope	$0.016 \pm 5(10)^{-4}$	-2.0	0.12	2.48
Constant pressure	$0.016 \pm 6(10)^{-5}$	-0.5	0.131	3.2
Pressure distribution I	$0.0184 \pm 5(10)^{-4}$	3.3	0.125	5.55
Pressure distribution II	$0.0147 \pm 5(10)^{-4}$	7.0	0.095	9.8

**** The value of S has been taken to be -3 for this case; this value is suggested as a limit on the analysis from a consideration of the shear stress profile given by Eq (10) as follows. It may be seen from Eq (10) that $(\tau/\tau_w) > 0$ for $\eta \ll 1$ and for $\eta \lesssim 1$ only if $S \gtrsim -3$. For $S \lesssim -3$ the shear would be negative in the outer part of the profile, and the velocity profile would have "overshoot." Since this is unacceptable for incompressible flows, the limit on S is taken to be -3. There does not seem to be a comparable limit on $S > 0$.

$\int_0^1 F dy$ This integral is $\varphi\Omega$ in the present notation, is Δ/δ according to Clauser, and is $A(\pi + 1)$, where π is the wake parameter of Coles.

respect to profiles and with respect to streamwise variations, and thus for providing the condition required to specify the shape parameters of the velocity profiles. The near constancy of the parameter β suggests that either of the two procedures just described for completing the system of equations for the direct problem will give equivalent results.

IV Conclusions

An analysis of the turbulent incompressible boundary layer with streamwise pressure gradients has been carried out. The analysis is applied to equilibrium and near-equilibrium flows, which have been obtained experimentally by others for adverse, zero, and favorable pressure gradients and which may be constructed numerically by application of the analysis. The results of these applications indicate that the suggestion of Clauser concerning the eddy viscosity in the outer layer incorporated in the present analysis provides a relatively simple, consistent, and accurate description of such flows. A means for determining the shape parameters of the velocity profiles for nonequilibrium flow is thus suggested.

References

- ¹ Clauser, F. H., "Turbulent boundary layers in adverse pressure gradients," *J. Aeronaut. Sci.* **21**, 91-108 (1954).
- ² Clauser, F. H., *The Turbulent Boundary Layer, Advances in Applied Mechanics* (Academic Press, New York, 1956), Vol. IV.
- ³ Coles, D., "The law of the wake in the turbulent boundary layer," *J. Fluid Mech.* **1**, 191-226 (1956).
- ⁴ Coles, D., "Remarks on the equilibrium turbulent boundary

layer," *J. Aeronaut. Sci.* **24**, 495-506 (1957).

⁵ Townsend, A. A., *The Structure of Turbulent Shear Flow* (Cambridge University Press, Cambridge, England, 1956).

⁶ Ferrari, C., Wall turbulence, *Corso Sulla Teoria della Turbolenza* (Casa Editrice Cremonesi, Rome, 1957), Sec. C; also NASA RE2 8-59W (March 1959).

⁷ Coles, D. E., "The turbulent boundary layer in a compressible fluid," Rand Corp. Rept. R-403-PR (September 1962).

⁸ Spence, D. A., "The development of turbulent boundary layers," *J. Aeronaut. Sci.* **23**, 31-15 (1956).

⁹ Rotta, J. C., "The turbulent boundary layers in incompressible flow," *Progress in Aeronautical Sciences* (Pergamon Press, New York, 1962), Vol. 2, pp. 1-220.

¹⁰ Coles, D., "The law of the wall in turbulent shear flow," *Jahre Grenzschichtforsch.* **50**, 133-163 (1955).

¹¹ Tetervin, N. and Lin, C. C., "A general integral form of the boundary layer equations for incompressible flow with an application to the calculation of the separation point of turbulent boundary layers," NACA TN 2158 (1950).

¹² Ludwig, H. and Tillman, W., "Untersuchungen über die Wandschubspannung in turbulenten Reibungsschichten," *Ingr.-Arch.* **17**, 288-299 (1949); also NACA TM 1285 (May 1950).

¹³ Libby, P. A., Baronti, P. O., and Napolitano, L., "A study of the turbulent boundary layer with pressure gradient, Part I, General analysis and equilibrium flows for incompressible fluids," General Applied Sci. Labs. Rept. 333 (February 1963).

¹⁴ Coles, D., "Measurements in the boundary layer on a smooth flat plate in supersonic flow, 1—The problem of the turbulent boundary layers," Jet Propulsion Lab., Calif. Inst. Tech. Rept. 20-69 (June 1, 1953).

¹⁵ Wieghardt, K. and Tillman, W., "Zur turbulenten Reibungsschicht Druckanstieg," *Deut. Luftfahrtforsch.* UM 6617 (November 20, 1944); also NACA TM 1314 (October 1951).

¹⁶ Bauer, W. J., "The development of the turbulent boundary layer on steep slopes," *Proc. Am. Soc. Civil Engrs.* **79**, no. 281, 1-25 (1953).

MARCH 1964

AIAA JOURNAL

VOL. 2, NO. 3

Nonequilibrium Hypersonic Flat-Plate Boundary-Layer Flow with a Strong Induced Pressure Field

GEORGE R. INGER*

Aerospace Corporation, El Segundo, Calif.

This paper presents a theoretical study of the effect of a strong self-induced pressure field on nonequilibrium hypersonic boundary-layer flow along a sharp flat plate in a dissociating diatomic gas. An analytical solution for the nearly frozen flow near the leading edge is presented which explicitly shows the effects of the induced pressure field in the case of strong interaction, including the back effect of the growing dissociation level on the induced pressure field itself. An approximate solution is also given for the entire nonequilibrium flow regime. The numerical results of the theory show that the induced pressure field can increase the degree of dissociation over a 10-ft run of plate by a factor of three to four or more at hypersonic flight conditions of practical interest. These results also suggest that the fully viscous flow region very near the leading edge can play an important part in determining the nonequilibrium dissociation history along the plate when the induced pressure field is taken into account.

Nomenclature

A = dissociation rate parameter
 C_∞ = Chapman-Rubens constant
 \bar{c}_p = frozen specific heat of mixture

D = dissociation rate distribution function [Eqs. (6) and (8)]
 F^* = function defined in Eq. (54)
 f = boundary layer stream function
 G = parameter in fully viscous flow theory [Eq. (57)]
 g = h/h
 g_w = $\bar{c}_p T_w / h$
 H_∞ = $2\alpha_\infty h_D / u_\infty^2$
 h_D = specific molecular dissociation energy
 h = total enthalpy
 I = integral in displacement thickness relation [Eqs. (11) and (14)]

Presented as Preprint 63-442 at the AIAA Conference on Physics of Entry into Planetary Atmospheres, Cambridge, Mass. August 26-28, 1963; revision received January 3, 1964.

* Member, Technical Staff, Aerodynamics and Propulsion Research Laboratory. Member AIAA.